

Error Rate Performance of Network–Coded Cooperative Diversity Systems

Amir Nasri[†], Robert Schober[†], and Murat Uysal^{††}

[†]University of British Columbia, Canada, ^{††}University of Waterloo, Canada

Abstract—In this paper, we study network–coded cooperative diversity (NCCD) systems comprising multiple sources, one relay, and one destination. The relay detects the packets received from all sources and performs Galois field network coding. We propose a simple cooperative maximum–ratio combining scheme for the destination which is shown to achieve the maximum diversity gain of the system. Furthermore, we provide a mathematical framework for the asymptotic analysis of NCCD systems with M –ary modulation for high signal–to–noise ratios. Based on this framework, we derive simple and elegant closed–form expressions for the asymptotic symbol and bit error rates which provide significant insight into the impact of various system and channel parameters on performance and can be exploited for performance optimization. Simulation results confirm the accuracy of the presented analysis and show that large performance gains are possible by optimizing the power allocation in NCCD systems based on the developed analytical results.

I. INTRODUCTION

Cooperative diversity (CD) is an effective technique to exploit the spatial diversity offered by wireless relay nodes. The main drawback of CD schemes is a reduction in throughput since the different cooperating terminals use orthogonal channels for transmission [1]. This throughput reduction is most noticeable in CD systems with multiple source terminals, since the relays forward the signals received by each source in a separate time slot or frequency band.

One effective approach to increase the throughput in multi–source CD systems is network coding [2]–[5]. The idea of network coding was originally developed for wired networks as an efficient routing technique capable of enhancing the network throughput [6]. However, network coding also allows a relay to first encode the packets received by several sources before forwarding a single encoded packet to the destination. Thus, the relay can simultaneously serve multiple sources and the network throughput is substantially increased.

The performance of the combination of CD and network coding, which is referred to as network–coded CD (NCCD), has been studied recently in the literature. In particular, the outage capacity and the diversity–multiplexing tradeoff of such a system was analyzed in [3] and [4], respectively, and its outage probability was calculated in [2]. Common to all these works is the assumption of error–free source–relay channels. Although this assumption greatly simplifies the analysis of NCCD systems, it may not be valid in practical wireless networks where detection errors at the relay may be caused by fading and noise. We also note that previous work on NCCD has focused on network coding over the Galois field (GF) of order two limiting the adopted modulation schemes to binary. Furthermore, a general and accurate error rate analysis giving insight into the performance of NCCD systems is not available in the literature.

In this paper, we consider an NCCD system with multiple sources using general M –ary modulation schemes, one

relay, and one destination. We propose a novel cooperative maximum–ratio combining (C–MRC) scheme at the destination, which guarantees full diversity for all sources even if the non–ideal detection at the relay is taken into account. The proposed C–MRC scheme may be viewed as a generalization of a similar scheme that was proposed for CD for a single source in [7]. Furthermore, we derive simple and elegant closed–form expressions for the asymptotic symbol and bit error rates of NCCD with C–MRC in Rayleigh fading. These closed–form expressions give valuable insight into the impact of various system and channel parameters such as the number of sources and the signal–to–noise ratios (SNRs) of the involved wireless channels. For example, our analytical results reveal that the diversity gain for all source terminals is two irrespective of the number of sources but the coding gain decreases as the number of sources increases. The derived error rate expressions can also be exploited for various NCCD system optimization problems such as optimal power allocation, relay selection, and relay placement.

The remainder of this paper is organized as follows. In Section II, the system model for the considered NCCD system as well as some notations and definitions are introduced. Asymptotic expressions for the symbol error rate (SER) and the bit error rate (BER) are derived in Section III. Numerical and simulation results are presented in Section IV, and conclusions are drawn in Section V.

II. PRELIMINARIES

In this section, we describe the model for the considered NCCD system and introduce some notations and definitions.

A. Notations and Definitions

In this paper, $[\cdot]^T$, $(\cdot)^*$, $\Re\{\cdot\}$, $\mathcal{E}_x\{\cdot\}$, and $\Gamma(\cdot)$, denote transposition, complex conjugation, the real part of a complex number, statistical expectation with respect to x , and the Gamma function, respectively. $Q(x) \triangleq \frac{1}{\sqrt{2\pi}} \int_x^\infty e^{-t^2/2} dt$ denotes the Gaussian Q –function. Furthermore, we use the notation $u \doteq v$ to indicate that u and v are asymptotically equivalent, and a function $f(x)$ is $o(g(x))$ if $\lim_{x \rightarrow 0} f(x)/g(x) = 0$.

B. Signal Model

The considered NCCD system is depicted in Fig. 1 and comprises N_s source terminals S_i , $1 \leq i \leq N_s$, one relay R , and one destination terminal D . Transmission from the source terminals to the destination terminal is organized in two hops. The first hop comprises N_s time slots and each source terminal S_i , $1 \leq i \leq N_s$, transmits a data packet to the relay and the destination using one time slot. In particular, the data symbol $s_i \in \mathcal{A}$ is generated at the source S_i , where $\mathcal{A} \triangleq \text{GF}(2^m)$ is the GF of order $M = 2^m$. Data symbol s_i is mapped to a transmit symbol $x_i \in \mathcal{X}$ with $\mathcal{E}\{|x_i|^2\} = 1$ using

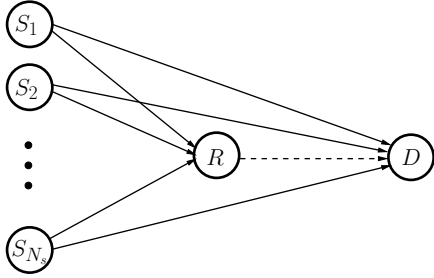


Fig. 1. Block diagram of the considered NCCD system. Solid and dashed lines denote links belonging to first and second hop, respectively.

the mapping $x_i = \mu_{\mathcal{X}}(s_i)$, where \mathcal{X} denotes an M -ary signal constellation such as M -ary phase-shift keying (M -PSK) and $\mu_{\mathcal{X}} : \mathcal{A} \rightarrow \mathcal{X}$ is a one-to-one mapping function from \mathcal{A} to \mathcal{X} . The transmit symbols x_i are transmitted to the relay and the destination. The signals received by the destination and the relay in the first hop are given by

$$r_{S_i D} = \sqrt{P_i} f_i x_i + n_{D,i}, \quad 1 \leq i \leq N_s, \quad (1)$$

and

$$r_{S_i R} = \sqrt{P_i} g_i x_i + n_{R,i}, \quad 1 \leq i \leq N_s, \quad (2)$$

respectively, where P_i is the average transmit power of the i th source, and f_i and g_i denote the fading gains of the $S_i \rightarrow D$ and the $S_i \rightarrow R$ channels, respectively. Furthermore, $n_{D,i}$ and $n_{R,i}$ denote the additive white Gaussian noise (AWGN) samples at the destination and the relay, respectively. The variances of these noise samples are denoted by $\sigma_{n_{D,i}}^2 \triangleq \mathcal{E}\{|n_{D,i}|^2\}$ and $\sigma_{n_{R,i}}^2 \triangleq \mathcal{E}\{|n_{R,i}|^2\}$, respectively.

Having received the signals $r_{S_i R}$ the relay performs coherent maximum-likelihood (ML) detection to obtain the detected symbols

$$\hat{x}_{R,i} = \arg \min_{\tilde{x} \in \mathcal{X}} \{|r_{S_i R} - \sqrt{P_i} g_i \tilde{x}|^2\}, \quad 1 \leq i \leq N_s. \quad (3)$$

The corresponding detected data symbol is given by $\hat{s}_{R,i} = \mu_{\mathcal{X}}^{-1}(\hat{x}_{R,i})$.

The second hop comprises a single time slot. In particular, the relay performs network coding and computes the data symbol $\hat{s}_R \triangleq \hat{s}_{R,1} \oplus \dots \oplus \hat{s}_{R,N_s} \in \mathcal{A}$, where \oplus denotes addition in $\text{GF}(2^m)$. The relay forwards transmit symbol $\hat{x}_R \triangleq \mu_{\mathcal{X}}(\hat{s}_R) \in \mathcal{X}$ to the destination. The signal received at the destination in the second hop, r_{RD} , can be modeled as

$$r_{RD} = \sqrt{P_R} h_R \hat{x}_R + n_{D,R}, \quad (4)$$

where P_R is the average transmit power of the relay, h_R is the fading gain of the $R \rightarrow D$ channel, and $n_{D,R}$ is the AWGN at the destination in the second hop having variance $\sigma_{n_{D,R}}^2 \triangleq \mathcal{E}\{|n_{D,R}|^2\}$.

Throughout this paper we assume independent Rayleigh fading for all links of the network. Thus, the fading gains $f_i \triangleq a_{f_i} e^{-j\theta_{f_i}}$, $h_i \triangleq a_{g_i} e^{-j\theta_{g_i}}$, $1 \leq i \leq N_s$, and $h_R \triangleq a_{h_R} e^{-j\theta_{h_R}}$, are independent Gaussian random variables (RVs) with zero mean and variances $\Omega_{f_i} \triangleq \mathcal{E}\{|f_i|^2\}$, $\Omega_{g_i} \triangleq \mathcal{E}\{|g_i|^2\}$, $1 \leq i \leq N_s$, and $\Omega_R \triangleq \mathcal{E}\{|h_R|^2\}$, respectively. Here, the channel amplitudes a_{f_i} , a_{g_i} , and a_{h_R} are positive real RVs and follow a Rayleigh distribution. Furthermore, the channel phases θ_{f_i} , θ_{g_i} , and θ_{h_R} are uniformly distributed in $[-\pi, \pi)$ and are independent from the channel amplitudes.

For future reference, we define the instantaneous SNRs of the $S_i \rightarrow D$, $S_i \rightarrow R$, and $R \rightarrow D$ links as $\gamma_{f_i} \triangleq$

$P_i a_{f_i}^2 / \sigma_{n_{D,i}}^2$, $\gamma_{g_i} \triangleq P_i a_{g_i}^2 / \sigma_{n_{R,i}}^2$, and $\gamma_{h_R} \triangleq P_R a_{h_R}^2 / \sigma_{n_{D,R}}^2$, respectively. The corresponding average SNRs are given by $\bar{\gamma}_{f_i} = P_i \Omega_{f_i} / \sigma_{n_{D,i}}^2$, $\bar{\gamma}_{g_i} = P_i \Omega_{g_i} / \sigma_{n_{R,i}}^2$, and $\bar{\gamma}_{D,R} = P_R \Omega_R / \sigma_{n_{D,R}}^2$, respectively.

Remark 1: Based on the presented signal model, a total of $N_s + 1$ time slots are required for the transmission of signals from all sources to the destination. In contrast, a conventional CD system [1], [7] requires $2N_s$ time slots since the relay assists only a single source at a time.

C. Equivalent Source-Relay Channel

Similar to conventional CD [7], it is also convenient for NCCD to introduce an equivalent channel between the source terminals and the relay. This will be particularly useful for the diversity combining scheme in Section II-D and the performance analysis in Section III. The input of this equivalent channel, x_R , is the relay transmit symbol in the absence of noise, i.e., $x_R \triangleq \mu_{\mathcal{X}}(s_R) \in \mathcal{X}$ with $s_R \triangleq s_1 \oplus \dots \oplus s_{N_s} \in \mathcal{A}$, and the output is the actual relay transmit symbol, $\hat{x}_R \in \mathcal{X}$. Defining the source-relay SNR vector $\gamma_g \triangleq [\gamma_{g_1}, \dots, \gamma_{g_{N_s}}]^T$, this channel is characterized by the equivalent error probability $P_{e,\text{eq}}(\gamma_g) \triangleq \Pr\{\hat{x}_R \neq x_R\}$. For an M -ary signal constellation \mathcal{X} , the equivalent error probability $P_{e,\text{eq}}(\gamma_g)$ is given by $P_{e,\text{eq}}(\gamma_g) = \beta Q(\sqrt{2\alpha\gamma_{\text{eq}}(\gamma_g)})$, where α and β are two modulation dependent constants (e.g. $\alpha = \beta = 1$ for BPSK) and $\gamma_{\text{eq}}(\gamma_g)$ is the instantaneous SNR associated with the equivalent source-relay channel. This equivalent SNR can be expressed as

$$\gamma_{\text{eq}}(\gamma_g) = \frac{1}{2\alpha} (Q^{-1}(P_{e,\text{eq}}(\gamma_g)/\beta))^2. \quad (5)$$

It can be shown that for sufficiently high SNR (please refer to Lemma 5 in the Appendix for a proof) $\gamma_{\text{eq}}(\gamma_g)$ can be accurately approximated as

$$\gamma_{\text{eq}}(\gamma_g) = \min\{\gamma_{g_1}, \dots, \gamma_{g_{N_s}}\}. \quad (6)$$

We note that since γ_{g_i} , $1 \leq i \leq N_s$, is an exponentially distributed RV with mean $\bar{\gamma}_{g_i}$, $\gamma_{\text{eq}}(\gamma_g)$ in (6) is also exponentially distributed with mean $\bar{\gamma}_{\text{eq}} = (1/\bar{\gamma}_{g_1} + \dots + 1/\bar{\gamma}_{g_{N_s}})^{-1}$.

D. Diversity Combining at the Destination

Due to the possibly erroneous decisions at the relay, the ML decision metric at the destination is highly complex and not amenable to analysis. In order to avoid the problems associated with the ML metric, we extend the C-MRC scheme proposed in [7] for conventional CD to NCCD. As will be shown in Section III, this simple C-MRC scheme achieves the full diversity of NCCD systems with any number of sources. The corresponding decision rule is given by

$$\hat{x}_D = \arg \min_{\tilde{x} \in \mathcal{X}^{N_s}} \{m_c(\tilde{x})\}, \quad (7)$$

Here, vector $\hat{x}_D \triangleq [\hat{x}_{D,1} \dots \hat{x}_{D,N_s}]^T \in \mathcal{X}^{N_s}$ contains the detected symbols at the destination for all sources, vector $\tilde{x} \triangleq [\tilde{x}_1 \dots \tilde{x}_{N_s}]^T \in \mathcal{X}^{N_s}$ contains trial transmit symbols $\tilde{x}_i = \mu_{\mathcal{X}}(\tilde{s}_i) \in \mathcal{X}$, $1 \leq i \leq N_s$, where $\tilde{s}_i \in \mathcal{A}$, $1 \leq i \leq N_s$, are trial data symbols, and $m_c(\tilde{x})$ is the C-MRC metric. The

decoded data symbols are obtained as $\hat{s}_{D,i} \triangleq \mu_{\mathcal{X}}^{-1}(\hat{x}_{D,i}) \in \mathcal{A}$, $1 \leq i \leq N_s$, and the C-MRC metric is given by

$$m_c(\tilde{\mathbf{x}}) = \sum_{i=1}^{N_s} \frac{|r_{S_i D} - \sqrt{P_i} f_i \tilde{x}_i|^2}{\sigma_{n_{D,i}}^2} + \lambda_R \frac{|r_{RD} - \sqrt{P_R} h_R \tilde{x}_R|^2}{\sigma_{n_{D,R}}^2} \quad (8)$$

where $\tilde{x}_R \triangleq \mu_{\mathcal{X}}(\tilde{s}_R) \in \mathcal{X}$ with $\tilde{s}_R \triangleq \tilde{s}_1 \oplus \cdots \oplus \tilde{s}_{N_s} \in \mathcal{A}$, and λ_R is a weighting factor which is defined as

$$\lambda_R \triangleq \frac{\min\{\gamma_{\text{eq}}(\gamma_g), \gamma_R\}}{\gamma_R}. \quad (9)$$

In order to compute λ_R , the receiver has to know the SNR of the weakest source-relay channel. This SNR can be measured at the relay and then forwarded to the destination over a low-rate feedback link. As mentioned before, the proposed C-MRC scheme is a generalization of the scheme in [7], which is obtained as a special case for $N_s = 1$, where NCCD reduces to conventional CD.

III. ASYMPTOTIC PERFORMANCE ANALYSIS

In this section, we analyze the asymptotic error rate performance of the considered NCCD system for high SNRs, i.e., $\bar{\gamma}_{f_i}, \bar{\gamma}_{g_i} \rightarrow \infty$, $1 \leq i \leq N_s$, and $\bar{\gamma}_R \rightarrow \infty$. In particular, we develop asymptotic closed-form expressions for the (average) pairwise error probability (PEP), SER, and BER.

For convenience, we introduce the source-destination SNR vector $\boldsymbol{\gamma}_f \triangleq [\gamma_{f_1}, \dots, \gamma_{f_{N_s}}]^T$, the normalized noise samples $\bar{n}_{D,i} \triangleq n_{D,i}/\sigma_{n_{D,i}}$, $1 \leq i \leq N_s$, and $\bar{n}_{D,R} \triangleq n_{D,R}/\sigma_{n_{D,R}}$, and noise vector $\mathbf{n} \triangleq [\bar{n}_{D,1}, \dots, \bar{n}_{D,N_s}, \bar{n}_{D,R}]^T$.

A. Asymptotic Pairwise Error Probability

Assuming that $\mathbf{x} \triangleq [x_1 \cdots x_{N_s}]^T \in \mathcal{X}^{N_s}$ was transmitted by the sources and $\tilde{\mathbf{x}} \triangleq [\tilde{x}_1 \cdots \tilde{x}_{N_s}]^T \in \mathcal{X}^{N_s}$, $\tilde{\mathbf{x}} \neq \mathbf{x}$, was detected at the destination, the PEP for the considered NCCD system can be expressed as

$$P(\mathbf{x} \rightarrow \tilde{\mathbf{x}}) = \Pr\{m_c(\mathbf{x}) > m_c(\tilde{\mathbf{x}})\}. \quad (10)$$

It is convenient to first obtain the PEP conditioned on the instantaneous SNRs $\gamma_f, \gamma_g, \gamma_R$, and the noise vector \mathbf{n} . This conditional PEP can be expressed as

$$P(\mathbf{x} \rightarrow \tilde{\mathbf{x}} | \boldsymbol{\gamma}_f, \boldsymbol{\gamma}_g, \gamma_R, \mathbf{n}) = [1 - P_{e,\text{eq}}(\boldsymbol{\gamma}_g)] P(\mathbf{x} \rightarrow \tilde{\mathbf{x}} | x_R, \boldsymbol{\gamma}_f, \gamma_{\text{eq}}, \gamma_R, \mathbf{n}) + \frac{1}{|\mathcal{N}(x_R)|} \sum_{\hat{x}_R \in \mathcal{N}(x_R)} P_{e,\text{eq}}(\boldsymbol{\gamma}_g) P(\mathbf{x} \rightarrow \tilde{\mathbf{x}} | \hat{x}_R, \boldsymbol{\gamma}_f, \gamma_{\text{eq}}, \gamma_R, \mathbf{n}) \quad (11)$$

where x_R and $P_{e,\text{eq}}(\boldsymbol{\gamma}_g)$ have been defined in Subsection II-C. In deriving (11), we have assumed that the erroneous $\hat{x}_R \in \mathcal{X}$ is a nearest neighbor of x_R , i.e., $\hat{x}_R \in \mathcal{N}(x_R)$, where set $\mathcal{N}(x_R)$ contains all nearest neighbors of x_R in \mathcal{X} . This approximation is well justified for $\bar{\gamma}_{g_i} \rightarrow \infty$, $1 \leq i \leq N_s$, and its accuracy will be confirmed by simulations in Section IV. The conditional PEP $P(\mathbf{x} \rightarrow \tilde{\mathbf{x}} | \bar{x}_R, \boldsymbol{\gamma}_f, \gamma_{\text{eq}}, \gamma_R, \mathbf{n})$, $\bar{x}_R \in \{x_R, \hat{x}_R\}$, can be expressed as

$$P(\mathbf{x} \rightarrow \tilde{\mathbf{x}} | \bar{x}_R, \boldsymbol{\gamma}_f, \gamma_{\text{eq}}, \gamma_R, \mathbf{n}) = \Pr\{m_c(\mathbf{x}) > m_c(\tilde{\mathbf{x}}) | \bar{x}_R, \boldsymbol{\gamma}_f, \gamma_{\text{eq}}, \gamma_R, \mathbf{n}\} = \Pr\left\{\sum_{i=1}^{N_s} \Delta_{f_i}(x_i, \tilde{x}_i) + \lambda_R \Delta_R(x_R, \tilde{x}_R, \bar{x}_R) < 0 \mid \boldsymbol{\gamma}_f, \gamma_{\text{eq}}, \gamma_R, \mathbf{n}\right\} \quad (12)$$

where

$$\Delta_{f_i}(x_i, \tilde{x}_i) \triangleq |\sqrt{\gamma_{f_i}}(x_i - \tilde{x}_i) + \bar{n}_{D,i}|^2, \quad (13)$$

and

$$\Delta_R(x_R, \tilde{x}_R, \bar{x}_R) \triangleq |\sqrt{\gamma_R}(x_R - \bar{x}_R) + \bar{n}_{D,R}|^2 - |\sqrt{\gamma_R}(\tilde{x}_R - \bar{x}_R) + \bar{n}_{D,R}|^2. \quad (14)$$

For derivation of the unconditional PEP, we exploit that for any RV Δ we have $\Pr\{\Delta < 0\} = \frac{1}{2\pi j} \int_{c-j\infty}^{c+j\infty} \Phi_{\Delta}(s) \frac{ds}{s}$ with moment generating function (MGF) $\Phi_{\Delta}(s) \triangleq \mathcal{E}_{\Delta}\{e^{-\Delta s}\}$ and $P_{e,\text{eq}}(\boldsymbol{\gamma}_g) = \beta Q(\sqrt{2\alpha \gamma_{\text{eq}}})$, cf. Subsection II-C. Using these relations, we obtain the unconditional PEP from (11) and (12) as

$$P(\mathbf{x} \rightarrow \tilde{\mathbf{x}}) = \mathcal{E}_{\boldsymbol{\gamma}_f, \boldsymbol{\gamma}_g, \gamma_R, \mathbf{n}}\{P(\mathbf{x} \rightarrow \tilde{\mathbf{x}} | \boldsymbol{\gamma}_f, \boldsymbol{\gamma}_g, \gamma_R, \mathbf{n})\} = \frac{1}{2\pi j} \int_{c-j\infty}^{c+j\infty} \left(\prod_{i=1}^{N_s} \Phi_{f_i}(s)\right) \Phi_R(s) \frac{ds}{s}, \quad (15)$$

where c is a small positive constant that lies in the region of convergence of the integrand and

$$\Phi_{f_i}(s) \triangleq \mathcal{E}_{\gamma_{f_i}, \bar{n}_{D,i}}\{e^{-s\Delta_{f_i}(x_i, \tilde{x}_i)}\}, \quad (16)$$

$$\Phi_R(s) \triangleq \Phi_R^c(s) + \frac{1}{|\mathcal{N}(x_R)|} \sum_{\hat{x}_R \in \mathcal{N}(x_R)} \Phi_R^e(\hat{x}_R; s). \quad (17)$$

Here, $\Phi_R^e(\hat{x}_R; s)$ and $\Phi_R^c(s)$ are defined in Lemmas 2 and 4 in the appendix, respectively.

Asymptotic expressions for the MGFs $\Phi_{f_i}(s)$, $\Phi_R^e(\hat{x}_R; s)$, and $\Phi_R^c(s)$ valid for high SNR are provided in the appendix in Lemmas 1, 2, and 4, respectively. With these asymptotic expressions for the MGFs at hand, an asymptotic result for the PEP $P(\mathbf{x} \rightarrow \tilde{\mathbf{x}})$ can be calculated based on (15). However, we postpone the derivation of the asymptotic PEP until Subsection III-B, since the computation of the asymptotic PEP depends on the actual values of \mathbf{x} and $\tilde{\mathbf{x}}$, which in turn depend on the considered signal constellation \mathcal{X} .

For derivation of the SER and BER, the following proposition is useful (please refer to the Appendix for a proof).

Proposition 1: Assume without loss of generality that $\bar{\gamma}_{f_i} = \zeta_{f_i} \bar{\gamma}$, $\bar{\gamma}_{g_i} = \zeta_{g_i} \bar{\gamma}$, $1 \leq i \leq N_s$, and $\bar{\gamma}_R = \zeta_R \bar{\gamma}$, where ζ_{f_i} , ζ_{g_i} and ζ_R are finite (positive) constants, which are independent of $\bar{\gamma}$, and define the diversity gain associated with the PEP as $G_{d,\text{PEP}} \triangleq -\lim_{\bar{\gamma} \rightarrow \infty} \log(P(\mathbf{x} \rightarrow \tilde{\mathbf{x}})) / \log(\bar{\gamma})$. The diversity gain is then given by $G_{d,\text{PEP}} = d_H(\mathbf{x}, \tilde{\mathbf{x}})$, where $d_H(\mathbf{x}, \tilde{\mathbf{x}})$ denotes the Hamming distance between data vector $\mathbf{s}_e \triangleq [s_1, \dots, s_{N_s}, s_R]^T$ and $\tilde{\mathbf{s}}_e \triangleq [\tilde{s}_1, \dots, \tilde{s}_{N_s}, \tilde{s}_R]^T$. Furthermore, for all possible pairs $(\mathbf{x}, \tilde{\mathbf{x}})$ we have $d_H(\mathbf{x}, \tilde{\mathbf{x}}) \geq 2$.

B. Asymptotic SER and BER

We use a truncated union-bound, where we include only nearest neighbor error events, to obtain an asymptotic expression for the SER based on the asymptotic PEP $P(\mathbf{x} \rightarrow \tilde{\mathbf{x}})$. In particular, a highly accurate approximation for the asymptotic SER of the i th source, P_s^i , is given by

$$P_s^i \triangleq \frac{1}{M^{N_s}} \sum_{\mathbf{x} \in \mathcal{X}^{N_s}} \sum_{\tilde{\mathbf{x}} \in \mathcal{C}_i(\mathbf{x})} P(\mathbf{x} \rightarrow \tilde{\mathbf{x}}), \quad (18)$$

where

$$\mathcal{C}_i(\mathbf{x}) \triangleq \{\tilde{\mathbf{x}} | \tilde{x}_j \in \mathcal{N}(x_j) \cup \{x_j\}, j \neq i, \tilde{x}_j \in \mathcal{N}(x_j), j = i, d_H(\mathbf{x}, \tilde{\mathbf{x}}) = 2\}. \quad (19)$$

TABLE I

COEFFICIENTS $C_{\mathcal{X}}^1$ AND $C_{\mathcal{X}}^2$ FOR DIFFERENT SIGNAL CONSTELLATIONS.

FOR M -PSK AND M -QAM WE HAVE $d = 2 \sin(\frac{\pi}{M})$,

$\nu \triangleq 4(\sin(\frac{2\pi}{M})^2 - \sin(\frac{\pi}{M})^2)$ AND $d = \sqrt{\frac{6}{M-1}}$, RESPECTIVELY.

\mathcal{X}	$C_{\mathcal{X}}^1$	$C_{\mathcal{X}}^2$
BPSK	$\frac{45+\sqrt{5}}{160}$	$\frac{3}{16}$
M -PSK	$\frac{8+\frac{2}{\sqrt{5}}}{d^4} + \frac{1-\sqrt{\frac{d^2}{d^2+4\nu}}}{d^2\nu}$	$\frac{6}{d^4}$
M -QAM	$\frac{18.27-\frac{17.44}{\sqrt{M}}-\frac{0.83}{\sqrt{M^3}}}{d^4}$	$\frac{12}{d^4} \left(1 - \frac{1}{\sqrt{M}}\right)$

In (19), we have only included error events with $d_H(\mathbf{x}, \tilde{\mathbf{x}}) = 2$ since error events with $d_H(\mathbf{x}, \tilde{\mathbf{x}}) > 2$ yield a higher diversity gain (cf. Proposition 1) and thus, their contribution to the asymptotic SER is negligible.

We are now ready to state our main result. In particular, in the following proposition we use (18) to obtain the asymptotic SER for BPSK, M -PSK, and M -QAM signal constellations.

Proposition 2: For an NCCD system with N_s sources the asymptotic SER for the i th source is given by

$$P_{s,\mathcal{X}}^i \triangleq \frac{1}{\bar{\gamma}_{f_i}} \left(C_{\mathcal{X}}^1 \sum_{i=1}^{N_s} \frac{1}{\bar{\gamma}_{g_i}} + C_{\mathcal{X}}^2 \left[\sum_{\substack{j=1 \\ j \neq i}}^{N_s} \frac{1}{\bar{\gamma}_{f_j}} + \frac{1}{\bar{\gamma}_R} \right] \right), \quad (20)$$

where $\mathcal{X} \in \{\text{BPSK}, M\text{-PSK}, M\text{-QAM}\}$, and $C_{\mathcal{X}}^1$ and $C_{\mathcal{X}}^2$ are tabulated in Table I.

Proof: The asymptotic SER $P_{s,\mathcal{X}}^i$ can be calculated by using (18) and (19) along with (15). Because of space limitations, we limit the proof to the BPSK case, i.e., $\mathcal{X} = \{\pm 1\}$. However, a similar approach can be used to obtain the SER for M -PSK, M -QAM, and any other signal constellation. In the BPSK case, for a given transmit signal vector \mathbf{x} , the set $\mathcal{C}_i(\mathbf{x})$ in (19) contains N_s elements, i.e., $\mathcal{C}_i(\mathbf{x}) = \{\tilde{\mathbf{x}}^1, \dots, \tilde{\mathbf{x}}^{N_s}\}$, $\tilde{\mathbf{x}}^l \triangleq [\tilde{x}_1^l, \dots, \tilde{x}_{N_s}^l]^T$, where

$$\tilde{x}_j^l = \begin{cases} -x_j, & j = i, j = l \\ x_j, & \text{otherwise} \end{cases}, \quad 1 \leq l \leq N_s, 1 \leq j \leq N_s. \quad (21)$$

In the following, we first obtain the asymptotic PEP $P(\mathbf{x} \rightarrow \tilde{\mathbf{x}}^l)$ for the case $l = i$ before we consider the case $l \neq i$.

Case 1 ($l = i$): Defining $d_j \triangleq |x_j - \tilde{x}_j^l|$, we have $d_j = 2$, $j = i$, and $d_j = 0$, $j \neq i$. As a result, from Lemma 1 we obtain $\Phi_{f_j}(s) \triangleq \frac{1}{4s(1-s)\bar{\gamma}_{f_j}}$, $j = i$ and $\Phi_{f_j}(s) \triangleq 1$, $j \neq i$. Furthermore, taking into account that for $l = i$ we have $\tilde{x}_R = -x_R$, based on Lemmas 2 and 4, (15), and (17) we obtain

$$P(\mathbf{x} \rightarrow \tilde{\mathbf{x}}^i) = \frac{1}{16\pi^2 j \bar{\gamma}_{f_i}} \int_0^{\pi/2} \int_{c-j\infty}^{c+j\infty} \frac{1}{s(1-s)} \times \left(\frac{1}{\bar{\gamma}_{\text{eq}} s (1 - 16 \sin^4 \theta s^2)} + \frac{1}{\bar{\gamma}_R s (1-s)} \right) \frac{ds}{s} d\theta, \quad (22)$$

where we have used that for BPSK $\mathcal{N}(x_R) = \{-x_R\}$, $\alpha = \beta = 1$, $\bar{d}_R(\tilde{x}_R) = -4$, and $d_R = 2$ are valid.

The inner complex integral in (22) can be calculated using the standard inverse Laplace transform techniques such as partial fraction expansion. This yields

$$P(\mathbf{x} \rightarrow \tilde{\mathbf{x}}^i) \triangleq \frac{1}{\bar{\gamma}_{f_i}} \left(C_{\text{BPSK}}^1 \sum_{i=1}^{N_s} \frac{1}{\bar{\gamma}_{g_i}} + C_{\text{BPSK}}^2 \frac{1}{\bar{\gamma}_R} \right), \quad (23)$$

where C_{BPSK}^1 and C_{BPSK}^2 are given in Table I.

Case 2 ($l \neq i$): For $l \neq i$, from Lemma 1 we have $\Phi_{f_j}(s) \triangleq \frac{1}{4s(1-s)\bar{\gamma}_{f_j}}$, $j = i, j = l$, and $\Phi_{f_j}(s) \triangleq 1$, otherwise. Furthermore, in this case $\tilde{x}_R = x_R$ is valid and therefore based on Lemmas 2 and 4 and (17) we have $\Phi_R(s) \triangleq 1$. Therefore, using (15) we arrive at

$$P(\mathbf{x} \rightarrow \tilde{\mathbf{x}}^l) = \frac{1}{32\pi j \bar{\gamma}_{f_i} \bar{\gamma}_{f_l}} \int_{c-j\infty}^{c+j\infty} \frac{1}{s^3(1-s)^2} ds = \frac{C_{\text{BPSK}}^2}{\bar{\gamma}_{f_i} \bar{\gamma}_{f_l}} \quad (24)$$

for $l \neq i, 1 \leq l \leq N_s$.

Finally, combining (18), (23), and (24) yields (20) for BPSK. ■

Remark 2: For $N_s = 1$ the considered NCCD system reduces to a CD system with a single decode-and-forward relay and C-MRC at the destination [7]. Letting $N_s = 1$ in (20), the asymptotic SER for this system can therefore be obtained as

$$P_{s,\mathcal{X}} \triangleq \frac{1}{\bar{\gamma}_{f_i}} \left(\frac{C_{\mathcal{X}}^1}{\bar{\gamma}_{g_i}} + \frac{C_{\mathcal{X}}^2}{\bar{\gamma}_R} \right), \quad (25)$$

which is a new result since the analysis presented in [7] reveals only the diversity gain but does not provide a tight approximation for the asymptotic SER.

We note that having obtained the asymptotic SER, for Gray labeling, the asymptotic BER of the i th source, $P_{b,\mathcal{X}}^i$, can be tightly approximated as

$$P_{b,\mathcal{X}}^i \triangleq \frac{1}{\log_2(M)} P_{s,\mathcal{X}}^i. \quad (26)$$

C. Diversity Gain and Coding Gain

Letting $\bar{\gamma}_{f_i} = \zeta_{f_i} \bar{\gamma}$, $\bar{\gamma}_{g_i} = \zeta_{g_i} \bar{\gamma}$, $1 \leq i \leq N_s$, and $\bar{\gamma}_R = \zeta_R \bar{\gamma}$, where ζ_{f_i} , ζ_{g_i} and ζ_R are finite (positive) constants, we can express the asymptotic SER of the i th source as $P_{s,\mathcal{X}}^i \triangleq (G_{c,\text{SER}}^i \bar{\gamma})^{-G_{d,\text{SER}}^i}$, where $G_{d,\text{SER}}^i$ and $G_{c,\text{SER}}^i$ are the diversity gain and the coding gain corresponding to the asymptotic SER, respectively. Thus, $G_{d,\text{SER}}^i$ and $G_{c,\text{SER}}^i$ correspond to the negative asymptotic slope and a relative horizontal shift of the SER curve when plotted as a function of $\bar{\gamma}$ on a double-logarithmic scale, respectively. Based on (20) we obtain $G_{d,\text{SER}}^i = 2$ and

$$G_{c,\text{SER}}^i[\text{dB}] = 5 \log_{10}(\zeta_{f_i}) - 5 \log_{10} \left(C_{\mathcal{X}}^1 \sum_{i=1}^{N_s} \zeta_{g_i}^{-1} + C_{\mathcal{X}}^2 \left[\sum_{\substack{j=1 \\ j \neq i}}^{N_s} \zeta_{f_j}^{-1} + \zeta_R^{-1} \right] \right). \quad (27)$$

Remark 3: A diversity gain of $G_{d,\text{SER}}^i = 2$ is achieved by all sources irrespective of the number of sources N_s . However, from (27) it is evident that the coding gain is dependent on the number of sources, the signal constellation \mathcal{X} , and the relative link qualities ζ_{f_i} , ζ_{g_i} , and ζ_R .

IV. RESULTS AND SYSTEM OPTIMIZATION

In this section, we verify the analytical results derived in Section III with computer simulations and exploit these results to optimize the performance of NCCD systems.

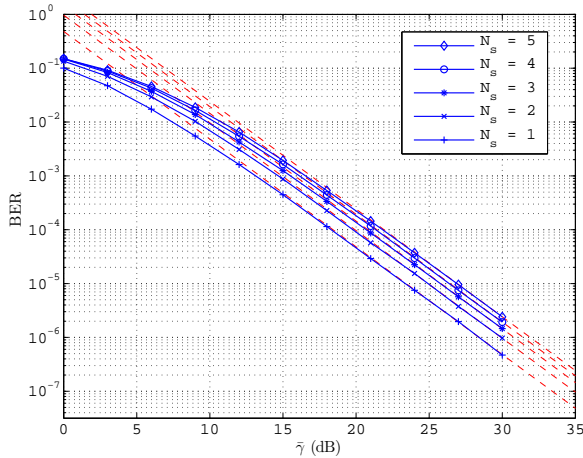


Fig. 2. Average BER vs. SNR $\bar{\gamma}$ of an NCCD system with N_s sources and BPSK. Solid lines with markers: Simulated BER. Dashed lines: Asymptotic BER [(20), (26)].

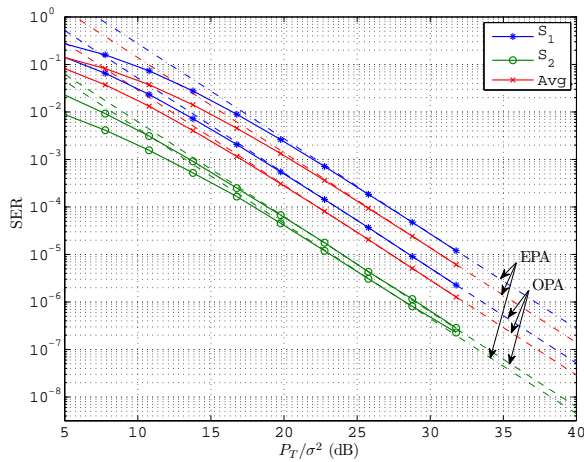


Fig. 3. SER vs. P_T/σ^2 of an NCCD system with 8-PSK for OPA and EPA. Solid lines with markers: Simulated SER. Dashed lines: Asymptotic SER [(20)].

A. Impact of Number of Sources

In Fig. 2, we show the average BER (average of the BERs of all sources) of an NCCD system for different numbers of sources as a function of $\bar{\gamma}$ for BPSK. $\zeta_{f_i} = \zeta_{g_i} = 1$, $1 \leq i \leq N_s$, $\zeta_R = 1$ are assumed, i.e., all links in the network have the same average quality. The analytical results (dashed lines) shown in Fig. 2 were obtained with (20) and (26) and are in excellent agreement with the simulation results (solid lines with markers) for sufficiently high SNR confirming the accuracy of the approximations made in Section II and III. As expected from the analysis in Section III, a diversity gain of two is achieved irrespective of N_s . However, increasing N_s causes a horizontal shift of the asymptotic BER and a performance degradation.

B. Performance Optimization

Similar to the case of conventional CD in [8], the asymptotic SER expression in (20) may be used for optimization of the NCCD system including optimal power allocation, relay selection, and relay placement. Because of space constraints, we only briefly discuss the power optimization problem here. Considering (20) and the definition of the SNRs $\bar{\gamma}_{g_i}$, $\bar{\gamma}_{f_i}$, $1 \leq i \leq N_s$, and $\bar{\gamma}_R$, it is obvious that the average SER

of all sources is a posynomial in the transmit powers P_i , $1 \leq i \leq N_s$, and P_R [9]. Thus, the problem of optimizing the transmit powers for minimization of the average SER under a joint transmit power constraint $\sum_{i=1}^{N_s} P_i + P_R \leq P_T$ (P_T : maximum transmit power) can be cast into a geometric program (GP) [9] as was done for conventional CD systems in [8]. Thus, the optimal power allocation (OPA) problem can be efficiently solved using standard tools [9].

Results for OPA as a function of P_T/σ^2 are shown in Fig. 3 for an NCCD system with 8-PSK, $N_s = 2$, $\Omega_{f_1} = \Omega_{g_1} = 1$, $\Omega_{f_2} = \Omega_{g_2} = 100$, $\Omega_R = 100$, and $\sigma_{n_{D,i}}^2 = \sigma_{n_{R,i}}^2 = \sigma_{n_{D,R}}^2 \triangleq \sigma^2$. Specifically, we show in Fig. 3 the SERs of both sources S_i , $i \in \{1, 2\}$ and the average SER of both sources, and compare OPA with equal power allocation (EPA), where $P_1 = P_2 = P_R = P_T/3$. Fig. 3 shows that OPA improves the average asymptotic SER (i.e., the cost function for optimization) by 3.4 dB compared to EPA. The individual SERs of S_1 and S_2 reveal that OPA improves the SER of S_1 , which has the weaker channel, at the expense of a small degradation of the SER of source S_2 by allocating more power to S_1 than to S_2 (and the relay).

V. CONCLUSIONS

In this paper, we studied NCCD with general M -ary modulation and proposed a simple C-MRC diversity combining scheme which achieves the maximum diversity of the considered system even if erroneous decisions at the relay are taken into account. Assuming independent Rayleigh fading for all links in the network, we derived closed-form expressions for the asymptotic SER and BER of the considered NCCD system. These simple and elegant expressions provide insight into the impact of various system and channel parameters on performance and can be exploited for performance optimization and system design. Simulation results confirmed the accuracy of the presented asymptotic SER and BER results and revealed that optimal power allocation can improve performance by several decibels.

APPENDIX

In this appendix, we prove Proposition 1 and provide lemmas 1–5.

Proof: [Proposition 1] Based on Lemma 1 $\Phi_{f_i}(s)$ can be written as $\Phi_{f_i}(s) \triangleq \tilde{k}_1 \bar{\gamma}$ for $x_i \neq \tilde{x}_i$ and $\Phi_{f_i}(s) \triangleq 1$ for $x_i = \tilde{x}_i$, where \tilde{k}_1 is a finite constant. Furthermore, using Lemmas 2 and 4 in (17) yields $\Phi_R(s) \triangleq \tilde{k}_2 \bar{\gamma}$ for $x_R \neq \tilde{x}_R$ and $\Phi_R(s) \triangleq \tilde{k}_3$ for $x_R = \tilde{x}_R$, where \tilde{k}_2 and \tilde{k}_3 are finite constants. Therefore, based on (15) we conclude that $G_{d,\text{PEP}}$ is given by the number of non-zero elements in the vector $[x_1 - \tilde{x}_1, \dots, x_{N_s} - \tilde{x}_{N_s}, x_R - \tilde{x}_R]^T$. Since $\mu_{\mathcal{X}} : \mathcal{A} \rightarrow \mathcal{X}$ is a one-to-one mapping function, $G_{d,\text{PEP}}$ is alternatively given by the Hamming distance between the transmit symbol vectors \mathbf{s}_e and $\tilde{\mathbf{s}}_e$ denoted as $d_H(\mathbf{x}, \tilde{\mathbf{x}})$. To see $d_H(\mathbf{x}, \tilde{\mathbf{x}}) \geq 2$, we first note that by definition we have $\mathbf{x} \neq \tilde{\mathbf{x}}$, and therefore $s_i \neq \tilde{s}_i$ is valid for $i \in \mathcal{I}$, where \mathcal{I} is a non-empty index set. For $|\mathcal{I}| \geq 2$, $d_H(\mathbf{x}, \tilde{\mathbf{x}}) \geq 2$ immediately follows. For $|\mathcal{I}| = 1$ it is easy to see that $s_R \neq \tilde{s}_R$, resulting in $d_H(\mathbf{x}, \tilde{\mathbf{x}}) = 2$. ■

Lemma 1: The asymptotic behavior of $\Phi_{f_i}(s)$, $1 \leq i \leq N_s$, for $\bar{\gamma}_{f_i} \rightarrow \infty$ is given by

$$\Phi_{f_i}(s) \triangleq \frac{1}{d_i^2 s (1-s) \bar{\gamma}_{f_i}}, \quad (28)$$

for $d_i \triangleq |x_i - \tilde{x}_i| \neq 0$ and $\Phi_{f_i}(s) \triangleq 1$ for $d_i = 0$.

Proof: For $d_i \neq 0$, following the same steps as in [10, Section IV.A] for $I_f(s) \triangleq \mathcal{E}_{\gamma_{f_i}} \{e^{-s\Delta_{f_i}(x_i, \tilde{x}_i)}\}$ we obtain

$$I_f(s) = \frac{1}{d_i^2 s \bar{\gamma}_{f_i}} \sum_{i=0}^{\infty} \frac{1}{i!} s^i |\bar{n}_{D,i}|^{2i} = \frac{e^{|\bar{n}_{D,i}|^2 s}}{d_i^2 s \bar{\gamma}_{f_i}}. \quad (29)$$

In particular, (29) can be obtained from [10, Eq. (14)] by adjusting the notation of [10] to the problem at hand. $\Phi_{f_i}(s) = \mathcal{E}_{\bar{n}_{D,i}} \{I_f(s)\}$ can then be calculated by averaging $I_f(s)$ with respect to the Rayleigh distributed RV $|\bar{n}_{D,i}|$ leading to the result in (28). For $d_i = 0$, $\Phi_{f_i}(s) \triangleq 1$ follows from the definition of $\Phi_{f_i}(s)$. ■

Lemma 2: The asymptotic behavior of $\Phi_R^c(\hat{x}_R; s) = \mathcal{E}_{\gamma_{\text{eq}}, \gamma_R, \bar{n}_{D,R}} \{\beta Q(\sqrt{2\alpha} \gamma_{\text{eq}}) e^{-s\lambda_R \Delta_R(x_R, \tilde{x}_R, x_R)}\}$ for $\bar{\gamma}_{g_i} \rightarrow \infty$, $1 \leq i \leq N_s$, and $\bar{\gamma}_R \rightarrow \infty$ is given by

$$\Phi_R^c(\hat{x}_R; s) \triangleq \frac{1}{\pi} \int_0^{\pi/2} \frac{\beta}{\bar{\gamma}_{\text{eq}}(\bar{d}_R(\hat{x}_R)s + \frac{\alpha}{\sin^2 \theta})} d\theta. \quad (30)$$

where $\bar{d}_R(\hat{x}_R) \triangleq |\tilde{x}_R - \hat{x}_R|^2 - |x_R - \hat{x}_R|^2$.

Proof: We start the proof by using the alternative representation of the Q -function, $Q(x) = \frac{1}{\pi} \int_0^{\pi/2} e^{-x^2/\sin^2 \theta} d\theta$, to express $\Phi_R^c(\hat{x}_R; s)$ as

$$\Phi_R^c(\hat{x}_R; s) = \frac{\beta}{\pi} \int_0^{\pi/2} \mathcal{E}_{\bar{n}_{D,R}} \{\Phi(s, \theta)\} d\theta, \quad (31)$$

where

$$\Phi(s, \theta) \triangleq \mathcal{E}_{\gamma_{\text{eq}}, \gamma_R} \left\{ e^{-\frac{\alpha \gamma_{\text{eq}}}{\sin^2 \theta}} e^{-s\lambda_R \Delta_R(x_R, \tilde{x}_R, \hat{x}_R)} \right\}. \quad (32)$$

Using the Taylor series expansion $e^x = \sum_{i=0}^{\infty} x^i/i!$ along with (9) and (14) in (32) leads to

$$\Phi(s, \theta) = \sum_{i=0}^{\infty} \frac{2^i \xi_i}{(2i)!} |\bar{n}_{D,R}|^{2i} s^{2i} \Psi_i(s, \theta), \quad (33)$$

where $\xi_i \triangleq \frac{\Gamma(i+1/2)}{\sqrt{\pi}\Gamma(i+1)}$ and $\Psi_i(s, \theta) = \Psi_i^1(s, \theta) + \Psi_i^2(s, \theta)$ with

$$\begin{aligned} \Psi_i^1(s, \theta) &\triangleq \frac{d_R^{2i}}{\bar{\gamma}_{\text{eq}} \bar{\gamma}_R} \int_0^{\infty} d\gamma_{\text{eq}} e^{-\left(\frac{\alpha \gamma_{\text{eq}}}{\sin^2 \theta} + \gamma_{\text{eq}}/\bar{\gamma}_{\text{eq}}\right)} \\ &\quad \times \int_0^{\gamma_{\text{eq}}} d\gamma_R \gamma_R^i e^{-(\gamma_R \bar{d}_R(\hat{x}_R)s + \gamma_R/\bar{\gamma}_R)}, \end{aligned} \quad (34)$$

$$\begin{aligned} \Psi_i^2(s, \theta) &\triangleq \frac{d_R^{2i}}{\bar{\gamma}_{\text{eq}} \bar{\gamma}_R} \int_0^{\infty} d\gamma_{\text{eq}} \gamma_{\text{eq}}^{2i} e^{-\gamma_{\text{eq}}(\bar{d}_R(\hat{x}_R) + \frac{\alpha}{\sin^2 \theta} + 1/\bar{\gamma}_{\text{eq}})} \\ &\quad \times \int_{\gamma_{\text{eq}}}^{\infty} d\gamma_R \gamma_R^{-i} e^{-(\gamma_R/\bar{\gamma}_R)}. \end{aligned} \quad (35)$$

In the following, we find the asymptotic behavior of $\Psi_i^1(s, \theta)$ and $\Psi_i^2(s, \theta)$ for $\bar{\gamma}_{\text{eq}}, \bar{\gamma}_R \rightarrow \infty$, respectively. We first write (34) as

$$\begin{aligned} \Psi_i^1(s, \theta) &= \frac{d_R^{2i}}{\bar{\gamma}_{\text{eq}} \bar{\gamma}_R} \int_0^{\infty} e^{-\left(\frac{\alpha \gamma_{\text{eq}}}{\sin^2 \theta} + \gamma_{\text{eq}}/\bar{\gamma}_{\text{eq}}\right)} \left[\frac{i!}{(\bar{d}_R(\hat{x}_R)s + 1/\bar{\gamma}_R)^{i+1}} \right. \\ &\quad \left. - \sum_{k=0}^i \frac{i! \gamma_{\text{eq}}^k e^{(\bar{d}_R(\hat{x}_R)s + 1/\bar{\gamma}_R)\gamma_{\text{eq}}}}{k! (\bar{d}_R(\hat{x}_R)s + 1/\bar{\gamma}_R)^{i-k+1}} \right] d\gamma_{\text{eq}} \\ &\triangleq o(\bar{\gamma}_{\text{eq}}^{-1} \bar{\gamma}_R^{-1}). \end{aligned} \quad (36)$$

Next, we rewrite (35) as

$$\Psi_i^2(s, \theta) = \frac{d_R^{2i}}{\bar{\gamma}_{\text{eq}} \bar{\gamma}_R} \int_0^{\infty} \gamma_{\text{eq}}^{2i} e^{-\gamma_{\text{eq}} A(s, \theta)} \Gamma(1-i, \gamma_{\text{eq}}/\bar{\gamma}_R) d\gamma_{\text{eq}}, \quad (37)$$

where $A(s, \theta) \triangleq \bar{d}_R(\hat{x}_R)s + \frac{\alpha}{\sin^2 \theta} + 1/\bar{\gamma}_{\text{eq}}$ and $\Gamma(\cdot, \cdot)$ is the incomplete Gamma function. Based on (37) and the asymptotic properties of $\Gamma(\cdot, z)$ for $z \rightarrow 0$, we obtain

$$\Psi_i^2(s, \theta) \triangleq \begin{cases} o(\bar{\gamma}_{\text{eq}}^{-1} \bar{\gamma}_R^{-1}) & i > 1 \\ \frac{2 \log(\bar{\gamma}_R)}{(A(s, \theta))^3 \bar{\gamma}_{\text{eq}} \bar{\gamma}_R} & i = 1 \\ \frac{1}{\bar{\gamma}_{\text{eq}}(\bar{d}_R(\hat{x}_R)s + \frac{\alpha}{\sin^2 \theta})} & i = 0 \end{cases} \quad (38)$$

From (37) and (38), we therefore obtain $\Psi_i(s, \theta) = \Psi_i^1(s, \theta) + \Psi_i^2(s, \theta) \triangleq \Psi_i^2(s, \theta)$. Substituting this result into (33) leads to (30) upon using (31). ■

Lemma 3: The asymptotic behavior of $I(s) \triangleq \mathcal{E}_{\gamma_{\text{eq}}, \gamma_R, \bar{n}_{D,R}} \{e^{-s\lambda_R \Delta_R(x_R, \tilde{x}_R, x_R)}\}$ for $\bar{\gamma}_{g_i} \rightarrow \infty$, $1 \leq i \leq N_s$, $\bar{\gamma}_R \rightarrow \infty$ is given by

$$I(s) \triangleq \frac{1}{\bar{\gamma}_{\text{eq}} d_R^2 s} - \frac{1}{\bar{\gamma}_R d_R^2 s(s-1)}, \quad (39)$$

for $d_R \triangleq |\tilde{x}_R - x_R| \neq 0$, while $I(s) = 1$ is valid for $d_R = 0$.

Proof: Since $\lambda_R \Delta_R(x_R, \tilde{x}_R, x_R) = \gamma_m d_R^2 + \frac{2\gamma_m}{\sqrt{\gamma_R}} d_R \Re\{\bar{n}_{D,R}^*\}$ with $\gamma_m \triangleq \min\{\gamma_{\text{eq}}, \gamma_R\}$, we conclude that $I(s) = 1$ is valid for $d_R = 0$. For $d_R \neq 0$ using a similar approach as in the proof of Lemma 2, we obtain

$$I(s|\bar{n}_{D,R}) = \mathcal{E}_{\bar{n}_{D,R}} \left\{ \sum_{i=0}^{\infty} \frac{2^i \xi_i}{(2i)!} |\bar{n}_{D,R}|^{2i} s^{2i} \Upsilon_i(s, \theta) \right\}, \quad (40)$$

where $\Upsilon_i(s, \theta) = \Upsilon_i^1(s, \theta) + \Upsilon_i^2(s, \theta)$ with

$$\Upsilon_i^1(s, \theta) \triangleq \frac{i!}{\bar{\gamma}_R d_R^2 s^{i+1}}, \quad \Upsilon_i^2(s, \theta) \triangleq \begin{cases} o(\bar{\gamma}_{\text{eq}}^{-1} \bar{\gamma}_R^{-1}) & i > 1 \\ \frac{2 \log(\bar{\gamma}_R)}{d_R^6 s^3 \bar{\gamma}_{\text{eq}} \bar{\gamma}_R} & i = 1 \\ \frac{1}{\bar{\gamma}_{\text{eq}} d_R^2 s} & i = 0 \end{cases} \quad (41)$$

We therefore arrive at

$$\Upsilon_i(s, \theta) \triangleq \begin{cases} \frac{i!}{\bar{\gamma}_R d_R^2 s^{i+1}} & i \geq 1 \\ \frac{1}{d_R^2 s} \left(\frac{1}{\bar{\gamma}_{\text{eq}}} + \frac{1}{\bar{\gamma}_R} \right) & i = 0 \end{cases} \quad (42)$$

Substituting (42) into (40) results in (39) upon averaging (40) over the Rayleigh distributed RV $|\bar{n}_{D,R}|$. ■

Lemma 4: The asymptotic behavior of $\Phi_R^c(s) \triangleq \mathcal{E}_{\gamma_{\text{eq}}, \gamma_R, \bar{n}_{D,R}} \{[1 - \beta Q(\sqrt{2\alpha} \gamma_{\text{eq}})] e^{-s\lambda_R \Delta_R(x_R, \tilde{x}_R, x_R)}\}$ for $\bar{\gamma}_{g_i} \rightarrow \infty$, $1 \leq i \leq N_s$, $\bar{\gamma}_R \rightarrow \infty$ is given by

$$\begin{aligned} \Phi_R^c(s) &\triangleq \frac{1}{\pi} \int_0^{\pi/2} \left(\frac{2}{\bar{\gamma}_{\text{eq}} d_R^2 s} - \frac{2}{\bar{\gamma}_R d_R^2 s(s-1)} \right. \\ &\quad \left. - \frac{\beta}{\bar{\gamma}_{\text{eq}} d_R^2 (s + \frac{\alpha}{\sin^2 \theta} d_R^2)} \right) d\theta, \end{aligned} \quad (43)$$

for $d_R \neq 0$, while $\Phi_R^c(s) \triangleq 1$ is valid for $d_R = 0$.

Proof: We first note that $\Phi_R^c(s) = I(s) - \Phi_R^e(x_R; s)$. For $d_R \neq 0$ combining (30) and (39) readily results in (43). For $d_R = 0$ from (30) and (39) we obtain $\Phi_R^c(s) = 1 - \frac{1}{\pi \bar{\gamma}_{\text{eq}}} \int_0^{\pi/2} \frac{\beta \sin^2 \theta}{\alpha} d\theta \triangleq 1$. ■

Lemma 5: For sufficiently high SNR $\gamma_{\text{eq}}(\gamma_g)$ given in (6) can be approximated as

$$\gamma_{\text{eq}}(\gamma_g) \approx \min\{\gamma_{g_1}, \dots, \gamma_{g_{N_s}}\}. \quad (44)$$

Proof: Since $\mu_{\mathcal{X}} : \mathcal{A} \rightarrow \mathcal{X}$ is a one-to-one mapping function the equivalent error probability $P_{e,\text{eq}}(\gamma_g) = \Pr\{\hat{x}_R \neq x_R\}$ is alternatively given by $P_{e,\text{eq}}(\gamma_g) = \Pr\{\mathcal{E}_e\}$,

where the error event \mathcal{E}_e is defined as $\mathcal{E}_e \triangleq \{\hat{s}_R \neq s_R\}$ with $\hat{s}_R = \hat{s}_{R,1} \oplus \cdots \oplus \hat{s}_{R,N_s}$ and $s_R = s_1 \oplus \cdots \oplus s_{N_s}$. For sufficiently high SNR the probability of \mathcal{E}_e is dominated by the probability of the event $\tilde{\mathcal{E}}_e = \bigcup_{i=1}^{N_s} \tilde{\mathcal{E}}_e^i$, where $\tilde{\mathcal{E}}_e^i$, $1 \leq i \leq N_s$, are mutually exclusive events defined as $\tilde{\mathcal{E}}_e^i \triangleq \{\hat{s}_{R,j} \neq s_j, j = i, \hat{s}_{R,j} = s_j, j \neq i\}$. We therefore can write

$$P_{e,\text{eq}}(\gamma_g) = \Pr\{\mathcal{E}_e\} \approx \Pr\{\tilde{\mathcal{E}}_e\} = \sum_{i=1}^{N_s} \Pr\{\tilde{\mathcal{E}}_e^i\}. \quad (45)$$

In the above equation $\Pr\{\tilde{\mathcal{E}}_e^i\}$ is given by

$$\begin{aligned} \Pr\{\tilde{\mathcal{E}}_e^i\} &= \beta Q\left(\sqrt{2\alpha\gamma_{g_i}}\right) \prod_{\substack{j=1 \\ j \neq i}}^{N_s} (1 - \beta Q(\sqrt{2\alpha\gamma_{g_j}})) \\ &\approx \beta Q(\sqrt{2\alpha\gamma_{g_i}}), \end{aligned} \quad (46)$$

where we have again used the sufficiently high SNR assumption to conclude $(1 - \beta Q(\sqrt{2\alpha\gamma_{g_j}})) \approx 1$. Based on (45), (46), and the alternative representation of the Q -function $Q(x) = \frac{1}{\pi} \int_0^{\pi/2} e^{-x^2/\sin^2\theta} d\theta$ we have

$$\begin{aligned} P_{e,\text{eq}}(\gamma_g) &\approx \frac{\beta}{\pi} \int_0^{\pi/2} \sum_{i=1}^{N_s} e^{-\frac{2\alpha\gamma_{g_i}}{\sin^2\theta}} d\theta \\ &\approx \frac{\beta}{\pi} \int_0^{\pi/2} e^{-\frac{2\alpha \min\{\gamma_{g_1}, \dots, \gamma_{g_{N_s}}\}}{\sin^2\theta}} d\theta \end{aligned} \quad (47)$$

$$= \beta Q\left(\sqrt{2\alpha \min\{\gamma_{g_1}, \dots, \gamma_{g_{N_s}}\}}\right), \quad (48)$$

where we have used the standard log-sum approximation in obtaining (47). Finally, using (48) in (6) leads to (44). ■

REFERENCES

- [1] J.N. Laneman, D.N.C. Tse, and G.W. Wornell. Cooperative Diversity in Wireless Networks: Efficient Protocols and Outage Behavior. *IEEE Trans. Inform. Theory*, 50:3062–3080, December 2004.
- [2] Y. Chen, S. Kishore, and J. Li. Wireless Diversity Through Network Coding. In *Proc. IEEE Wireless Commun. and Networking Conf. (WCNC)*, volume 3, pages 1681–1686, 2006.
- [3] M. Yu, J. Li, and R.S. Blum. User Cooperation Through Network Coding. In *Proc. IEEE Inter. Conf. Commun. (ICC)*, pages 4064–4069, 2007.
- [4] C. Peng, Q. Zhang, M. Zhao, Y. Yao, and W. Jia. On the Performance Analysis of Network-Coded Cooperation in Wireless Networks. *IEEE Trans. Wireless Commun.*, 7:3090–3097, August 2008.
- [5] Z. Han, X. Zhang, and H.V. Poor. High Performance Cooperative Transmission Protocols Based on Multiuser Detection and Network Coding. *IEEE Trans. Wireless Commun.*, 8:2352–2361, May 2009.
- [6] R. Ahlswede, N. Cai, S. Li, and R. Yeung. Network Information Flow. *IEEE Trans. Inform. Theory*, 46:1204–1216, July 2000.
- [7] T. Wang, A. Cano, G.B. Giannakis, and J.N. Laneman. High-Performance Cooperative Demodulation With Decode-and-Forward Relays. *IEEE Trans. Commun.*, 55:1427–1438, July 2007.
- [8] A. Nasri, R. Schober, and I.F. Blake. Performance and Optimization of Cooperative Diversity Systems in Generic Noise and Interference. *Submitted to the IEEE Trans. Wireless Commun.*, available at: <http://www.ece.ubc.ca/~amirn/TW09.pdf>, 2010.
- [9] S. Boyd and L. Vandenberghe. *Convex Optimization*. Cambridge, U.K.: Cambridge Univ. Press, 2004.
- [10] A. Nasri and R. Schober. Performance of BICM-SC and BICM-OFDM Systems with Diversity Reception in Non-Gaussian Noise and Interference. *IEEE Trans. Commun.*, pages 3316–3327, November 2009.